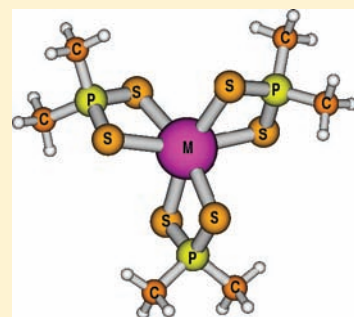


Selective Americium(III) Complexation by Dithiophosphinates: A Density Functional Theoretical Validation for Covalent Interactions Responsible for Unusual Separation Behavior from Trivalent Lanthanides

Arunasis Bhattacharyya,[†] Tapan Kumar Ghanty,[‡] Prasanta Kumar Mohapatra,^{*,†} and Vijay Kumar Manchanda[†]

[†]Radiochemistry Division and [‡]Theoretical Chemistry Section, Bhabha Atomic Research Centre, Mumbai-400085, India

ABSTRACT: The separation of trivalent actinides and lanthanides is a challenging task for chemists because of their similar charge and chemical behavior. Soft donor ligands like Cyanex-301 were found to be selective for the trivalent actinides over the lanthanides. Formation of different extractable species for Am³⁺ and various lanthanides (viz. La³⁺, Eu³⁺, and Lu³⁺) was explained on the basis of their relative stabilities as compared to their corresponding trinitrato complexes calculated using the density functional method. Further, the metal–ligand complexation energy was segregated into electrostatic, Pauli repulsion, and orbital interaction components. Higher covalence in the M–S bond in the dithiophosphinate complexes as compared to the M–O bond in the nitrate complexes was reflected in the higher orbital and lower electrostatic interactions for the complexes with increasing number of dithiophosphinate ligands. Higher affinity of the dithiophosphinate ligands for Am³⁺ over Eu³⁺ was corroborated with higher covalence in the Am–S bond as compared to the Eu–S bond, which was reflected in shorter bond length in the case of the former and higher ligand to metal charge transfer in Am(III)–dithiophosphinate complexes. The results were found to be consistent in gas phase density functional theory (DFT) calculations using different GGA functional. More negative complexation energies in the case of Eu³⁺ complexes of Me₂PS₂[−] as compared to the corresponding Am³⁺ complexes in spite of marginally higher covalence in the Am–S bond as compared to the Eu–S bond might be due to higher ionic interaction in the Eu³⁺ complexes in the gas phase calculations. The higher covalence in the Am–S bond obtained from the gas phase studies of their geometries and electronic structures solely cannot explain the selectivity of the dithiophosphinate ligands for Am³⁺ over Eu³⁺. Presence of solvent may also play an important role to control the selectivity as observed from higher complexation energies for Am³⁺ in the presence of solvent. Thus, the theoretical results were able to explain the experimentally observed trends in the metal–ligand complexation affinity.



INTRODUCTION

In the PUREX process, the long-lived minor actinides (MAs) such as ²³⁷Np, ²⁴¹Am, ²⁴³Am, and ²⁴⁵Cm along with the different fission product elements (FPs) are left behind in the raffinate which are subsequently concentrated to yield the high level waste (HLW) stream. Though the geologic disposal of vitrified HLW has been the accepted strategy at present, partitioning of the long-lived MA and fission products from HLW followed by their transmutation in high flux reactors or accelerator driven subcritical systems (ADSS) is evolving as the alternative strategy for the mitigation of the long-term risks arising from their large radiotoxicity. For this purpose, a number of partitioning processes (e.g., TRUEX, TRPO, DIDPA, and DIAMEX) have been developed during the last two decades for the partitioning of actinides from the bulk of short-lived and inactive material.^{1,2} None of these processes can distinguish between the trivalent trans-plutonides (Am³⁺, Cm³⁺, etc.) and the lanthanides due to their similar charge to radius ratio which results in similar electrostatic interaction with hard O donor ligands. This leads to the coextraction of trivalent lanthanides along with the

trivalent MAs. There is a need to separate Ln(III) from An(III) in view of the larger amount of lanthanides (20–50 times depending on the burn up) over that of the minor actinides and high neutron absorption cross section of some isotopes of lanthanides. The latter is relevant during the transmutation of long-lived radionuclides in high energy high flux reactors or ADSS as it may render the transmutation process of minor actinides inefficient. Additionally, during target preparation for transmutation, lanthanides do not form solid solutions with MAs and segregates in separate phases with the tendency to grow under thermal treatments.

It is desirable, therefore, to develop suitable complexing agents which can differentiate between the trivalent actinides and lanthanides mainly based on the softer nature of the trivalent actinides vis-à-vis the trivalent lanthanides. The actinides are capable of forming stronger covalent bonds with the soft donor ligands as compared to the lanthanides. This property is

Received: November 8, 2010

Published: March 30, 2011

universally exploited for their mutual separation. Diamond et al. separated Am^{3+} from Pm^{3+} in strong HCl medium using cation exchange resin, where Pm^{3+} is held and Am^{3+} is washed out because of formation of anionic chloride complex of Am^{3+} .³ Subsequently, Moore has separated trivalent actinides and lanthanides using an anion exchange column by forming anionic chloride or thiocyanate complexes of actinides in strong chloride or thiocyanate media due to the soft donor nature of Cl^- or SCN^- , where lanthanides form only a neutral complex.^{4,5} This concept was used in the well-known TRAMEX process for Ln/An separation.⁶ Earlier, Musikas has shown stronger complexation of trivalent actinides with the N_3^- ion⁷ and various heteropolycyclic N donor ligands, viz. terpyridine, 2,4,6-tri(2-pyridyl)-1,3,5-triazine (TPTZ), 2,6-di(5-alkyl-1,2,4-triazol-3-yl)-pyridine, and 2,6-di(5,6-dialkyl-1,2,4-triazine-3-yl)pyridine (BTP).⁸ Basicity of these ligands is less due to the involvement of the lone pairs of N atoms in the aromatic rings but due to their chelating nature they show high complexing power with the actinides. These ligands can, therefore, extract actinides from low pH medium.

Among various N donor ligands reported, bis-triazinylpyridines (BTPs) and bis-triazinylbipyridines (BTBPs) were found to be most promising for Ln/An separation under acidic conditions (at low pH conditions). All of these ligands show maximum separation factor ($D_{\text{An}}/D_{\text{Ln}}$) of ~ 100 . In 1996, Zhu et al. have reported a separation factor (S.F.) of 5900 using a S donor ligand, bis(2,4,4-trimethylpentyl)dithiophosphinic acid (Cyanex-301).⁹ A number of reports appeared subsequently on the separation of actinides and lanthanides employing Cyanex-301 as the extractant.^{10–12} In order to enhance the extractability, some O donor neutral ligands, viz. tri-*n*-butyl phosphate (TBP), tri-*n*-octyl phosphine oxide (TOPO), etc., were introduced along with Cyanex-301, but with increasing basicity of O donor ligands, the S.F. values decreased.¹³ The reason for the reduction of selectivity was attributed to weakening of the metal–Cyanex-301 bond with increasing basicity of the O donor ligands.¹⁴ Employing N donor neutral ligands along with Cyanex-301, beside the extraction of actinides, selectivity was also enhanced due to the soft donor nature of both the ligands.¹⁵ Reports are also available on the structural and spectroscopic studies of the lanthanide and actinide complexes of Cyanex-301 to understand the reason behind such a high selectivity of Cyanex-301 for trivalent actinides over the lanthanides.^{16,17} Jensen et al. did not find any structural difference in the extracted complexes of Cm^{3+} and Sm^{3+} using Cyanex-301 in *n*-dodecane medium, and the selectivity was attributed to an increased covalence in the An–S bonds which was, however, not reflected in shorter An–S bonds.¹⁶ Tian et al., however, found different extractable species for lighter lanthanides (La^{3+} , Nd^{3+} , Eu^{3+}) and Am^{3+} from the EXAFS, ESI-MS, and IR studies.¹⁷ A number of papers are available on the theoretical studies of the lanthanide complexes of thiophosphinate ligands.^{18–20} To the best of our knowledge, only one report appeared in the literature very recently on the comparative studies of Am^{3+} , Cm^{3+} , and Eu^{3+} complexation by Cyanex-301.²¹ They suggested that the desolvation energy of the metal ions plays a significant role in their extraction behavior. From the solvent extraction study, we have observed different extractable species for Am^{3+} and Eu^{3+} , which of course are very much dependent on the Cyanex-301 concentration in the organic phase and the presence of NaNO_3 in the aqueous phase.²² It is therefore of interest to study the extractable species of lighter as well as heavier lanthanides using Cyanex-301 and compare them with that of Am^{3+} . A systematic study was,

therefore, carried out on the extraction of Am^{3+} , La^{3+} , Eu^{3+} , and Lu^{3+} with varying Cyanex-301 concentrations in the presence of 1 M NaNO_3 in the aqueous phase. The experimental results were also supported by the computational studies, where the binding energies of different possible species of Am^{3+} and the three lanthanides were calculated using DFT with various functionals and their energy decomposition analysis was carried out in order to understand the bonding in the complexes. Partial atomic charges were also calculated in their complexes using Mulliken population analysis and natural population analysis (NPA). Effect of the solvent was also studied on the structure, energetics, and charge distribution of those complexes.

EXPERIMENTAL SECTION

Reagents. Commercial Cyanex-301 supplied by Cytec Canada Inc. was purified by the reported method,⁹ and the purity was checked by ³¹P NMR, GC-MS, and elemental analysis. Sulphanilic acid was procured from Sisco Research Laboratory (SRL), Mumbai, and was used as such. ²⁴¹Am was purified as reported earlier,²³ and the purity was checked by alpha spectrometry. ^{152,154}Eu was procured from Board of Radiation and Isotope Technology (BRIT), Mumbai, India. ¹⁴⁰La and ¹⁷⁷Lu were produced by irradiating natural isotopes of La and Lu in APSARA reactor in BARC. Suprapure nitric acid (Merck) was used for preparing the tracer solutions. All other reagents were of AR grade.

Distribution Studies. Distribution studies were carried out using ²⁴¹Am, ¹⁴⁰La, ^{152,154}Eu, and ¹⁷⁷Lu tracers under varying experimental conditions. Solutions of desired concentrations of Cyanex-301 in toluene were used as the organic phase while the aqueous phase contained a mixture of 1 M NaNO_3 and 0.02 M sulphanilic acid (which acted as the buffer) at a pH value of 3.4 for Am^{3+} and 4.5 for the lanthanides. Extremely low *D* values of the lanthanides at pH 3.4 necessitated the use of higher aqueous phase pH for obtaining measurable *D* values. Equal volumes (1.0 mL) of the organic phase and the aqueous phase containing the required tracer at the desired pH were kept for equilibration in a thermostatted water bath. The tubes were equilibrated at constant temperature (25 ± 0.1 °C) for 30 min, though less than 10 min was required to attain equilibrium. The two phases were then centrifuged and assayed by taking suitable aliquots (100–200 μL) from both the phases. The gamma activities were measured using a NaI(Tl) scintillation detector. The distribution ratio (D_M) was calculated as the ratio of counts per minute per unit volume in the organic phase to that in the aqueous phase. Mass balance was within the experimental error limits ($\pm 5\%$).

Computational Studies. $\text{Me}_2\text{PS}_2\text{H}$ was chosen as a model compound for Cyanex-301 since its selectivity for trivalent actinides over the lanthanides does not change with increasing the alkyl chain length.¹⁸ $\text{Me}_2\text{PS}_2\text{H}$, therefore, as a representative molecule for Cyanex-301 helps to reduce the computational difficulties. The density functional theory was found to be an effective tool for the description of ground states of the *f*-elements when applied with the scalar relativistic ZORA approach and the Becke–Perdew GGA functional.^{24–26} The geometries of the molecules were, therefore, optimized at the GGA level of DFT by using Becke's exchange functional²⁷ in conjunction with Perdew's correlation functional²⁸ (BP86) with generalized gradient approximation (GGA). The functionals used for the DFT calculations have a strong influence on the geometrical parameters, energetics, and atomic charge distribution in the complexes of the *f* elements.^{29,30} Vetere et al. have done extensive studies on the bonding of the trivalent actinide and lanthanide complexes using various pure (BP86, PBE) and hybrid (PBE0, B3LYP, B1LYP) DFT functionals and found that the results obtained using the pure GGA functionals are more reliable as compared to that of the hybrid one.^{31,32} Calculations were, therefore, also

performed using other pure GGA functionals, viz. PW91,³³ BLYP,^{27,34} and PBE³⁵ in order to check the consistency of the results with respect to various exchange correlation functionals. Uncontracted Slater-type orbitals (STOs) were employed as basis functions (basis set B1) in SCF calculations.³⁶ Triple- ζ -quality basis sets were used, which were augmented by two sets of polarization functions (p and d functions for the hydrogen atom and d and f functions for the other atoms) for the description of the valence part of all atoms. We kept their core frozen up to 4d for lanthanides; 5d for americium; 2p for phosphorus and sulfur; and 1s for carbon, nitrogen, and oxygen. Scalar relativistic effects were considered by using the zero-order regular approximation (ZORA).^{37–41} The atomic partial charges were calculated using the Mulliken population analysis.⁴² These calculations were carried out with the ADF package (program release 2006.01).^{42–44} The theoretical treatment of trivalent f element complexes with ADF has been investigated several times by various research groups.^{24,31,45,46} The bonding interactions between the fragments, viz. M^{3+} ion and a combination of three ligands [$n\text{Me}_2\text{PS}_2^- + (3-n)\text{NO}_3^-$ with $n = 0–3$], have been analyzed with the energy decomposition scheme of the program package ADF,⁴² which is based on the generalized transition-state method developed by Ziegler and co-workers.⁴⁷ The total bond dissociation energy ΔE_n ($n =$ number of Me_2PS_2^- ion, present in the complex, varying from 0 to 3 in our case) between the fragments is partitioned into several contributions which can be identified as physically meaningful quantities. First, ΔE_n is separated into two major components, ΔE_{prep} and ΔE_{int} :

$$\Delta E_n = \Delta E_{\text{prep}} + \Delta E_{\text{int}} \quad (1)$$

ΔE_{prep} is the preparatory energy, which is needed to promote the fragments from their equilibrium geometry to that in the respective complexes. In the gas phase calculations, the bare metal ion does not require any desolvation energy prior to its complexation with the ligands, and no preparatory energy is, therefore, required for its complexation. ΔE_{int} is the instantaneous interaction energy between the two fragments in the complex, and this quantity is the focus of the bonding analysis. This interaction energy ΔE_{int} can be divided into different components:

$$\Delta E_{\text{int}} = \Delta E_{\text{steric}} + \Delta E_{\text{orb}} \quad (2)$$

ΔE_{steric} is the steric interaction energy between the metal and the three ligands, and it arises from the sum of two contributions:

$$\Delta E_{\text{steric}} = \Delta E_{\text{elec}} + \Delta E_{\text{pauli}} \quad (3)$$

ΔE_{elec} gives the electrostatic interaction energy between the fragments which are calculated with a frozen electron density distribution in the geometry of the complex. ΔE_{pauli} gives the repulsive interactions between the fragments which are caused by the fact that two electrons with the same spin cannot occupy the same region in space. The term comprises the four-electron destabilizing interactions between occupied orbitals. The stabilizing orbital interaction term ΔE_{orb} is calculated in the final step of the analysis when Kohn–Sham orbitals relax to their final form. The basis set superposition error (BSSE) was found to be very small (<1%) as compared to the complexation energies,^{24,25} and it was, therefore, neglected all through the calculations. All the calculations on solvent effects were carried out using the COSMO approach⁴⁸ with the TURBOMOLE program package⁴⁹ where for the heavy atoms 46 (La), 28 (Eu and Lu), and 60 (Am) electron core pseudopotentials (ECPs) along with the corresponding def-SV(P) basis set (basis set B2) were selected. All other lighter atoms were treated at the all electron (AE) level, and the standard def-SV(P) basis sets as implemented in the TURBOMOLE program was used. It may be noted that for the Am and Eu atoms the def-SV(P) basis set as present in the TURBOMOLE basis set library is quite large and consists of (14s13p10d8f1g) functions contracted to [10s9p5d4f1g].^{50–56} The dielectric constants (ϵ 's) of water and toluene were considered as 78.4 and 2.38, respectively. For the

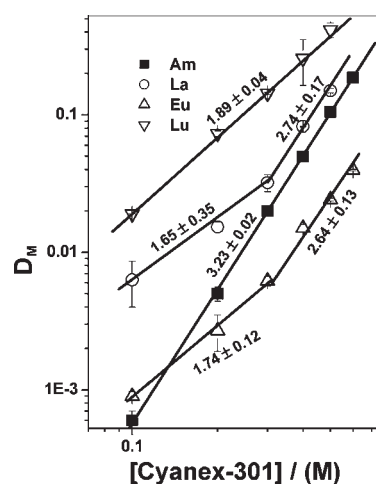


Figure 1. Effect of Cyanex-301 concentration on the distribution ratio of Am^{3+} and different lanthanide ions: organic phase Cyanex-301 in toluene; aqueous phase 0.02 M sulphanic acid buffer at pH 3.4 for Am^{3+} and pH 4.5 for the lanthanides containing 1 M NaNO_3 .

cavity generation, the following atomic radii (Å) were used in COSMO calculations: C, 1.989; H, 1.404; O, 1.778; N, 1.778; S, 2.106; P, 2.106; Eu, 1.820; Am, 2.045;²¹ La, 1.856; and Lu, 1.655.⁵⁷ The charge distribution in Am^{3+} and Eu^{3+} complexes in the gas phase as well as in the presence of solvent were calculated by natural population analysis in TURBOMOLE.

RESULTS AND DISCUSSION

Distribution Studies. Solvent extraction studies of Am^{3+} and three representative lighter to heavier lanthanides, viz. La^{3+} , Eu^{3+} , and Lu^{3+} , were carried out varying the Cyanex-301 concentration from 0.1 to 0.5 M in toluene medium using 0.02 M sulphanic acid at pH 3.4 for Am^{3+} and pH 4.5 for the lanthanides as the aqueous phase. The ionic strength was maintained constant at 1 M NaNO_3 throughout in the present work. Sulphanic acid was chosen as the buffering agent as it does not complex with the lanthanides and actinides.⁵⁸ In the case of lighter lanthanides, viz. La^{3+} and Eu^{3+} , the slope of the logarithmic plot of D_{Ln} versus Cyanex-301 concentration was found to be ~ 2 up to 0.3 M Cyanex-301, and it increased to ~ 3 at higher Cyanex-301 concentration. In case of Lu^{3+} and Am^{3+} , the observed slope values were 1.89 ± 0.04 and 3.23 ± 0.02 , respectively, in the whole Cyanex-301 concentration range studied (Figure 1). This observation suggests that, in case of La^{3+} and Eu^{3+} , the extractable species contain 2 molecules of Cyanex-301 and the residual charge was neutralized by one nitrate ion. This is because only neutral species can be extracted in the nonpolar solvent like toluene, and NO_3^- is present in much larger concentration as compared to the metal ion, thereby forming a species of the type $\text{LnA}_2(\text{NO}_3)$ (where HA is Cyanex-301). However, with increasing Cyanex-301 concentration beyond 0.3 M, the nitrate ion is further replaced by another Cyanex-301 resulting in a species of the type LnA_3 , but for Lu^{3+} , the $\text{LuA}_2(\text{NO}_3)$ type of species was extracted in the whole Cyanex-301 concentration range studied. In the case of Am^{3+} , the extractable species of the type AmA_3 remained unchanged in the whole Cyanex-301 concentration range studied. A similar kind of species, LnA_3 , was observed by Jensen et al. with the help of XAFS, when they extracted Nd^{3+} and Sm^{3+} using 0.5 M Cyanex-301 in n-dodecane medium.¹⁶

Table 1. Calculated Bond Lengths (Å) in Various Stoichiometric Complexes of Am^{3+} , La^{3+} , Eu^{3+} , and Lu^{3+} with Me_2PS_2^- and NO_3^- using Different GGA Exchange Correlation Functionals and Basis Set B1 using ADF Program

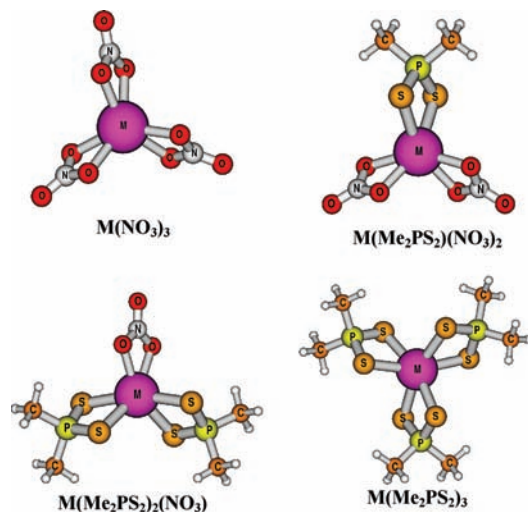
complex	$d_{(\text{M-S})}$					$d_{(\text{M-O})}$				
	BP86	BP86 ^a	PW91	BLYP	PBE	BP86	BP86 ^a	PW91	BLYP	PBE
$\text{Am}(\text{NO}_3)_3$						2.408	2.388	2.403	2.433	2.406
$\text{La}(\text{NO}_3)_3$						2.462	2.495	2.458	2.487	2.460
$\text{Eu}(\text{NO}_3)_3$						2.399	2.391	2.395	2.422	2.398
$\text{Lu}(\text{NO}_3)_3$						2.260	2.245	2.256	2.278	2.260
$\text{Am}(\text{Me}_2\text{PS}_2)(\text{NO}_3)_2$	2.786	2.782	2.778	2.831	2.778	2.427	2.403	2.422	2.454	2.426
$\text{La}(\text{Me}_2\text{PS}_2)(\text{NO}_3)_2$	2.877	2.923	2.869	2.916	2.869	2.491	2.512	2.478	2.507	2.481
$\text{Eu}(\text{Me}_2\text{PS}_2)(\text{NO}_3)_2$	2.814	2.826	2.803	2.861	2.805	2.406	2.401	2.409	2.435	2.412
$\text{Lu}(\text{Me}_2\text{PS}_2)(\text{NO}_3)_2$	2.663	2.657	2.658	2.694	2.660	2.280	2.262	2.276	2.299	2.280
$\text{Am}(\text{Me}_2\text{PS}_2)_2(\text{NO}_3)$	2.820	2.813	2.810	2.867	2.811	2.437	2.408	2.432	2.466	2.435
$\text{La}(\text{Me}_2\text{PS}_2)_2(\text{NO}_3)$	2.904	2.944	2.895	2.943	2.895	2.494	2.525	2.491	2.519	2.493
$\text{Eu}(\text{Me}_2\text{PS}_2)_2(\text{NO}_3)$	2.835	2.843	2.824	2.881	2.826	2.422	2.411	2.419	2.447	2.423
$\text{Lu}(\text{Me}_2\text{PS}_2)_2(\text{NO}_3)$	2.682	2.680	2.685	2.726	2.687	2.294	2.276	2.290	2.315	2.294
$\text{Am}(\text{Me}_2\text{PS}_2)_3$	2.838	2.829	2.827	2.890	2.830					
$\text{La}(\text{Me}_2\text{PS}_2)_3$	2.920	2.953	2.911	2.961	2.911					
$\text{Eu}(\text{Me}_2\text{PS}_2)_3$	2.850	2.860	2.839	2.899	2.842					
$\text{Lu}(\text{Me}_2\text{PS}_2)_3$	2.714	2.705	2.705	2.752	2.710					

^a Using TURBOMOLE program with basis set B2.

Tian et al.,¹⁷ however, have observed an extractable species of the type $\text{HLnA}_4 \cdot \text{H}_2\text{O}$ for La^{3+} , Nd^{3+} , and Eu^{3+} . They used Cyanex-301 saponified up to 25 mol % with 4 M NaOH, and the complexable anionic Cyanex-301 was much higher as compared to the present work.

Computational Studies. Bidentate coordination mode of nitrate ion was considered for all the calculations as the stability of the lanthanide complex is higher when the nitrate ion coordinates in bidentate mode.⁵⁹ Jensen and Bond have shown from the XAFS study that Cyanex-301 coordinates as a bidentate chelating ligand through both the S atoms forming a four-membered chelate ring.¹⁶ We, therefore, considered Me_2PS_2^- (model compound for Cyanex-301 used in the calculations) as the bidentate ligand in all the calculations. Various calculated parameters are discussed in the following sections.

Geometry Optimization. Metal–ligand bond distances were calculated for all the possible complexes of Am^{3+} , La^{3+} , Eu^{3+} , and Lu^{3+} with different stoichiometries of NO_3^- and Me_2PS_2^- ions after optimization of their geometries using the septet state for Am^{3+} , Eu^{3+} and singlet state in the case of La^{3+} , Lu^{3+} (Table 1). In all the complexes, Ln–O (for NO_3^-) and Ln–S (for Me_2PS_2^-) bond distances were found to decrease by ~ 0.2 Å from La^{3+} to Lu^{3+} . On comparison of the ionic radii of the lanthanides, the size of Lu^{3+} is found to be smaller than that of La^{3+} by 0.184 Å,⁶⁰ and it matches closely with our results. In the free ligand, Me_2PS_2^- , the P–S bond distance was found to be 2.015 Å. This indicates that very weak double bond character is present in the P–S bond, and various literature reports also show that the extremely small π component is present in the P–S bonds.⁶¹ The P–S bond length increased further to 2.04 Å upon complexation with Am^{3+} or Lu^{3+} ions. This certainly indicates that the electron donation from the S to the P atom decreased because of transfer of electron density from S to the metal ions, resulting in further reduction in bond order as compared to the free Me_2PS_2^- ion. A similar observation was also reported by Boehme and Wipff for the complexation of Ph_2PS_2^- , where the

**Figure 2.** Representative structures of NO_3^- and Me_2PS_2^- complexes of Am^{3+} and Ln^{3+} ions in different stoichiometries.

P–S bond length increased from 2.012 to 2.125 Å in the $[\text{Ph}_2\text{PS}_2\text{Yb}]^{2+}$ complex.¹⁸ In that complex the increase is much higher as compared to our results as they have considered the interaction of Yb^{3+} ion with one Ph_2PS_2^- ion, whereas in our case three anions are present and the overall interaction is distributed among the three ligands resulting in less transfer of electron density from each individual ligand. Structures of representative complexes of NO_3^- and Me_2PS_2^- with Am^{3+} and Ln^{3+} ions in different stoichiometries are shown in Figure 2. An interesting result was obtained when the M–O and M–S bond distances were compared in the NO_3^- and Me_2PS_2^- complexes of Am^{3+} and Eu^{3+} ions. M–O bond distances in all the NO_3^- complexes were found to be lower in the case of Eu^{3+} as compared to Am^{3+} , whereas the Am–S bonds were

Table 2. Interaction Energies (ΔE_{int}), Ligand Preparatory Energies (ΔE_{prep}), and Complexation Energies ($\Delta E_n = \Delta E_{\text{int}} + \Delta E_{\text{prep}}$) in kcal mol⁻¹ of Am³⁺ and Lanthanide Ions in the NO₃⁻ and Me₂PS₂⁻ Complexes of Different Stoichiometry^a

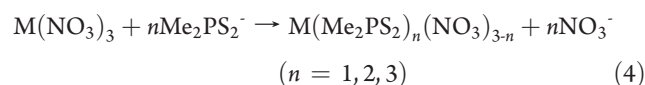
complex	ΔE_{int}	ΔE_{prep}	ΔE_n
Am(NO ₃) ₃	-1207.5	220.2	-987.3
La(NO ₃) ₃	-1157.8	215.6	-942.3
Eu(NO ₃) ₃	-1237.2	218.7	-1018.6
Lu(NO ₃) ₃	-1272.2	235.4	-1036.9
Am(Me ₂ PS ₂)(NO ₃) ₂	-1210.2	215.8	-994.4
La(Me ₂ PS ₂)(NO ₃) ₂	-1156.2	210.5	-945.8
Eu(Me ₂ PS ₂)(NO ₃) ₂	-1238.7	214.7	-1024.0
Lu(Me ₂ PS ₂)(NO ₃) ₂	-1269.9	227.9	-1042.0
Am(Me ₂ PS ₂) ₂ (NO ₃)	-1209.1	212.1	-997.1
La(Me ₂ PS ₂) ₂ (NO ₃)	-1153.6	206.7	-946.9
Eu(Me ₂ PS ₂) ₂ (NO ₃)	-1237.2	211.3	-1025.9
Lu(Me ₂ PS ₂) ₂ (NO ₃)	-1265.0	222.3	-1042.7
Am(Me ₂ PS ₂) ₃	-1206.8	209.8	-997.1
La(Me ₂ PS ₂) ₃	-1150.3	203.9	-946.4
Eu(Me ₂ PS ₂) ₃	-1234.2	208.9	-1025.3
Lu(Me ₂ PS ₂) ₃	-1258.3	218.7	-1039.6

^a Calculations were performed using exchange-correlation functional BP86 and basis set B1 and ADF program.

shorter as compared to the Eu–S bonds in the Me₂PS₂⁻ complexes although the size of the Am³⁺ ion is slightly larger than the Eu³⁺ ion. This shows higher interaction of the Me₂PS₂⁻ ligand with Am³⁺ as compared to the Eu³⁺ ion. Geometries of all the complexes of Am³⁺, La³⁺, Eu³⁺, and Lu³⁺ with NO₃⁻ and Me₂PS₂⁻ ligands were also optimized using other pure GGA level of density functionals, and the metal–ligand bond distances were found to be in good agreement with the functional BP86. The shorter Am–S bond length as compared to the Eu–S bond was also observed with different functionals. Geometries of the Am³⁺ and Eu³⁺ complexes [M(SH)²⁺] with a simple S donor anionic ligand (SH⁻) were optimized using the exchange correlation functional BP86 and basis set A in ADF. Similar to the Me₂PS₂⁻ ligand, a shorter Am–S bond (2.785 Å) as compared to the Eu–S bond (2.895 Å) and less Mulliken charge on Am (1.59) as compared to Eu (1.64) were observed here reflecting the higher covalence in the Am–S bond as compared to the Eu–S one. The difference in Am–S and Eu–S bond distance is much smaller (<0.03 Å) in the case of Me₂PS₂⁻ complexes (Table 1) as compared to the complexes with simple SH⁻ ion (0.11 Å) which might be due to the higher steric hindrance in the case of Me₂PS₂⁻ complexes. No structural difference was, however, seen by Jensen and Bond¹⁶ using XAFS studies in the Cyanex-301 complexes of Cm³⁺ and Sm³⁺. They have also interpreted this effect due to the possible steric interactions between three Cyanex-301 ligands because of the presence of bulkier 2,4,4-trimethylpentyl groups which were replaced by smaller methyl groups in our calculations, resulting in a marginally shorter Am–S bond as compared to the Eu–S bond.

Energetics of the Ln³⁺ Complexes and Rationalization of the Experimental Results. The interaction energy, ΔE_{int} , of the Ln³⁺ ions in the complexes studied in the present work became more negative as we went along the series (Table 2). This is because of the fact that along the lanthanide series the ionic potential

increases resulting in an increase in electrostatic attraction with the anionic ligands. Preparatory energy, ΔE_{prep} , increases for the higher lanthanide complexes due to the decrease in size of the Ln³⁺ ions along the series, thereby increasing the interligand repulsion. For a particular Ln³⁺ ion, if we go on replacing the NO₃⁻ with Me₂PS₂⁻ ions, ΔE_{prep} decreased, as we can see that ΔE_{prep} value decreased from 215.6 to 203.9 kcal mol⁻¹ when all the three NO₃⁻ ions in La(NO₃)₃ were replaced by three Me₂PS₂⁻ ions. This is because of higher repulsive interactions among the NO₃⁻ ions due to their close proximity as compared to the bulkier Me₂PS₂⁻ ion. The complexation energy, ΔE_n , was calculated according to eq 1, and the values are listed in Table 3. In spite of higher preparatory energies, ΔE_n values are more negative for the higher lanthanides in all the four complexes of different stoichiometries. Similar trends for Ln³⁺ ions were also reported by Boehme and Wipff, where they have calculated the complexation energies of the lanthanide complexes of the type Ln(Me₂PS₂)₂²⁺ for La³⁺, Eu³⁺, and Yb³⁺, which were found to be -490.9, -522.8, and -548.0 kcal mol⁻¹, respectively.¹⁸ More negative ΔE_n or ΔE^{int} values in the case of Eu³⁺ complexes of Me₂PS₂⁻ as compared to the corresponding Am³⁺ complexes in spite of marginally higher covalence in the Am–S bond as compared to the Eu–S bond might be due to higher ionic interaction in the Eu³⁺ complexes. The higher covalence in the Am–S bond obtained from the gas phase studies of their geometries and electronic structures solely cannot explain the selectivity of the dithiophosphinate ligands for Am³⁺ over Eu³⁺. Presence of solvent may also play an important role to control the selectivity as described by Cao et al.²¹ The experimental results on the stoichiometries of the extractable complexes of Am³⁺ and lanthanide ions by Cyanex-301 can be rationalized by these complexation energies (ΔE_n). The relative stabilities of Me₂PS₂⁻ complexes of Am³⁺ and Ln³⁺ ions compared to the NO₃⁻ complexes, M(NO₃)₃, were calculated from the change in complexation energies with respect to the NO₃⁻ complex ($\Delta E_r = \Delta E_n - \Delta E_o$). ΔE_r can also be called a reaction energy for the following chemical reaction (eq 4), and are values listed in Table 3.



In general, for the lanthanides, the ΔE_r value was found to be most negative for $n = 2$, but in the case of early lanthanides, viz. La³⁺ and Eu³⁺, ΔE_r values are very close for $n = 2$ and 3. Therefore, both the M(Me₂PS₂)₂(NO₃) and M(Me₂PS₂)₃ species are of comparable stability. Their extractable species can, therefore, be altered depending on the relative proportion of the two complexing anions present in the medium. From the experimental studies using the solvent extraction technique it was also found that these two lanthanide ions are extracted as Ln(Cyanex-301)₂(NO₃) or Ln(Cyanex-301)₃ depending on the Cyanex-301 concentration present in the organic phase. In the case of Lu³⁺, the ΔE_r value is more negative for $n = 2$ as compared to that for $n = 3$, and the difference in ΔE_r value for $n = 2$ and 3 is higher as compared to that in the cases of La³⁺ and Eu³⁺. Hence, Lu(Me₂PS₂)₂(NO₃) is, therefore, the most stable complex for Lu³⁺, and experimentally, it was also observed to be extracted as Lu(Cyanex-301)₂(NO₃) irrespective of the Cyanex-301 concentration studied in the present work. The ΔE_r values for $n = 1$ (-5.1 kcal.mol⁻¹) and $n = 2$ (-5.8 kcal.mol⁻¹) are very

Table 3. Complexation ($\Delta E_n = \Delta E_{\text{int}} + \Delta E_{\text{prep}}$) and Reaction ($\Delta E_r = \Delta E_n - \Delta E_0$) Energies in kcal mol⁻¹ of Different Me₂PS₂⁻ and NO₃⁻ Complexes of Am³⁺ and Ln³⁺ Ions (eq 4) using Different GGA Level of Exchange Correlation Functionals^a

M ³⁺	complex	n	ΔE_n				ΔE_r			
			BP86	PW91	BLYP	PBE	BP86	PW91	BLYP	PBE
Am ³⁺	Am(NO ₃) ₃	0	-987.3	-994.1	-977.1	-991.9	0	0	0	0
Am ³⁺	Am(Me ₂ PS ₂)(NO ₃) ₂	1	-994.4	-1001.7	-982.2	-999.5	-7.4	-7.6	-5.1	-7.6
Am ³⁺	Am(Me ₂ PS ₂) ₂ (NO ₃)	2	-997.1	-1004.8	-982.8	-1002.6	-9.8	-10.7	-5.7	-10.8
Am ³⁺	Am(Me ₂ PS ₂) ₃	3	-997.1	-1005.6	-980.3	-1003.3	-9.8	-11.5	-3.3	-11.4
La ³⁺	La(NO ₃) ₃	0	-942.3	-949.3	-931.8	-947.6	0	0	0	0
La ³⁺	La(Me ₂ PS ₂)(NO ₃) ₂	1	-945.8	-953.3	-933.6	-951.6	-3.5	-4.0	-1.8	-4.0
La ³⁺	La(Me ₂ PS ₂) ₂ (NO ₃)	2	-946.9	-954.9	-932.8	-953.3	-4.6	-5.6	-1.0	-5.7
La ³⁺	La(Me ₂ PS ₂) ₃	3	-946.4	-954.9	-929.8	-953.2	-4.1	-5.6	2.0	-5.6
Eu ³⁺	Eu(NO ₃) ₃	0	-1018.6	-1022.5	-1006.5	-1020.3	0	0	0	0
Eu ³⁺	Eu(Me ₂ PS ₂)(NO ₃) ₂	1	-1024.0	-1028.3	-1010.4	-1026.1	-5.4	-5.8	-4.0	-5.8
Eu ³⁺	Eu(Me ₂ PS ₂) ₂ (NO ₃)	2	-1025.9	-1030.7	-1010.4	-1028.5	-7.3	-8.2	-4.0	-8.2
Eu ³⁺	Eu(Me ₂ PS ₂) ₃	3	-1025.3	-1030.8	-1007.4	-1028.5	-6.7	-8.3	-0.9	-8.2
Lu ³⁺	Lu(NO ₃) ₃	0	-1036.9	-1044.7	-1031.0	-1042.4	0	0	0	0
Lu ³⁺	Lu(Me ₂ PS ₂)(NO ₃) ₂	1	-1042.0	-1050.4	-1034.0	-1048.1	-5.1	-5.6	-3.0	-5.7
Lu ³⁺	Lu(Me ₂ PS ₂) ₂ (NO ₃)	2	-1042.7	-1051.7	-1032.0	-1049.5	-5.8	-7.0	-1.0	-7.2
Lu ³⁺	Lu(Me ₂ PS ₂) ₃	3	-1039.6	-1049.7	-1025.8	-1047.3	-2.7	-5.0	5.2	-5.0

^a Calculations were performed using the basis set B1 and ADF program.

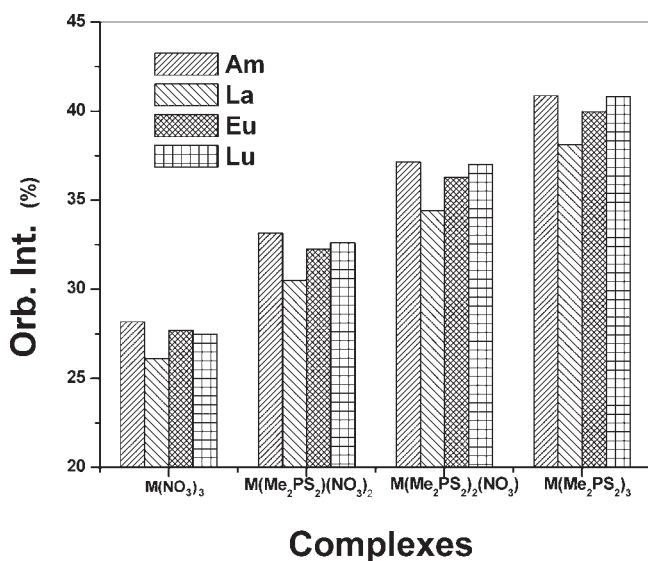


Figure 3. Percentage contribution of orbital interactions (ΔE_{orb}) in the total interaction energies (ΔE_{int}) for the Am³⁺ and Ln³⁺ complexes in different stoichiometric proportion of NO₃⁻ and Me₂PS₂⁻ ions.

close in the case of Lu³⁺. Both the species Lu(Cyanex-301)-(NO₃)₂ and Lu(Cyanex-301)₂(NO₃) are, therefore, formed, but the greater hydrophobicity of the latter one makes it the major extractable species of Lu³⁺ in the organic phase as observed from the slope analysis method of the solvent extraction study. In the case of Am³⁺, the ΔE_r value was similar for $n = 2$ and 3 ; hence, they are of similar stability. The species with $n = 3$ possesses more lipophilicity, and Am(Cyanex-301)₃, therefore, is the main extractable species for Am³⁺ in the solvent extraction studies (Figure 1). ΔE_n and ΔE_r were also calculated for all the complexes of Am³⁺ and three lanthanides using other density functionals (PW91, BLYP, and PBE), and similar trends were

observed in their values except the ΔE_r for $n = 3$ was less negative as compared to $n = 1$ and 2 for Am³⁺ using the density functional BLYP. It was also interesting to note that the reaction energy (ΔE_r) was more negative in case of Am³⁺ as compared to the lanthanides. This indicates that Me₂PS₂⁻ ligand has more affinity toward Am³⁺ over the lanthanides than the nitrate ion resulting in higher selectivity of Me₂PS₂⁻ for Am³⁺ over the lanthanides.

The interaction energies, ΔE_{int} 's, were decomposed into orbital and steric interactions. It is interesting to note that, for Am³⁺ and all the lanthanide ions studied here, the percentage of orbital interaction (ΔE_{orb}) in the total interaction energy (ΔE_{int}) increases as we go on increasing the number of Me₂PS₂⁻ ions at the cost of NO₃⁻ ions (Figure 3). Higher orbital interactions reveal higher covalence in the metal–ligand bond. Me₂PS₂⁻ forms stronger covalent M–S bonds with the Am³⁺ and lanthanide ions as compared to the M–O bonds with NO₃⁻ ion, and it is clearly reflected in the higher orbital interactions with increasing the number of Me₂PS₂⁻ and decreasing the number of NO₃⁻ ions in the complexes. It is also interesting to note that the contribution of orbital interaction is higher in case of Am³⁺ complexes as compared to the respective Eu³⁺ complexes, which indicates higher covalent interactions in the Me₂PS₂⁻ complexes of Am³⁺ as compared to the Eu³⁺ complexes. Dithiophosphate ligands, therefore, show very high selectivity toward the Am³⁺ ion over the Eu³⁺ ion. The orbital interaction (ΔE_{orb}) consists of two terms, viz. a polarization term (ΔE_{pol}) caused by reorganization of metal and ligand electronic densities during complexation and a covalence term due to the metal–ligand orbital overlap, and these two terms can not be resolved in ADF.²⁴ The higher ΔE_{orb} for Lu³⁺ complexes could be due to the higher contribution from ΔE_{pol} because of higher charge density in the Lu³⁺ ion. The percentage of steric interaction in the total interaction energies was found to decrease with an increase in the number of Me₂PS₂⁻ ligands and a decrease in the number of NO₃⁻ ions in the complexes (Figure 4).

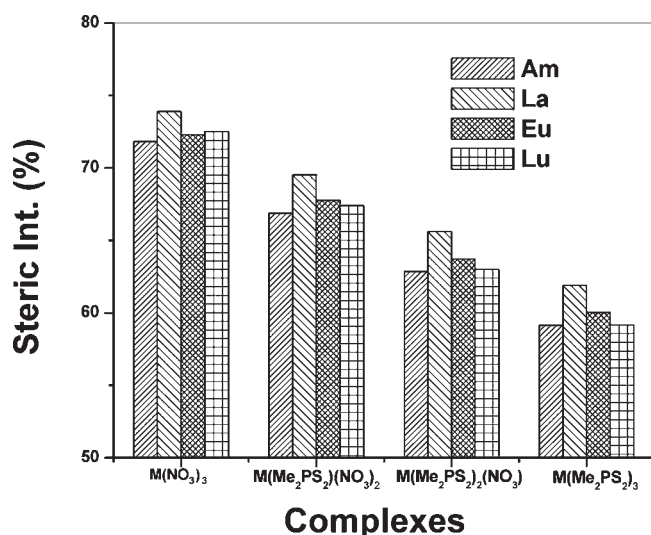


Figure 4. Percentage contribution of steric interactions (ΔE_{steric}) in the total interaction energies (ΔE_{int}) for the Am^{3+} and Ln^{3+} complexes in different stoichiometric proportion of NO_3^- and Me_2PS_2^- ions.

Table 4. Mulliken Charges on the Metal Ions (Using Four Different Exchange Correlation Functionals) and Transfer of Charges (Using the DFT Functional BP86) from the NO_3^- [$\Delta Q(\text{NO}_3^-)$] and Me_2PS_2^- [$\Delta Q(\text{Me}_2\text{PS}_2^-)$] Ligands to the Metal Ion in Different Am^{3+} and Ln^{3+} Complexes^a

complex	Q(M)				ΔQ	ΔQ
	BP86	PW91	BLYP	PBE	(NO_3^-)	(Me_2PS_2^-)
$\text{Am}(\text{NO}_3)_3$	1.70	1.69	1.72	1.68	0.43	
$\text{La}(\text{NO}_3)_3$	1.64	1.60	1.67	1.60	0.45	
$\text{Eu}(\text{NO}_3)_3$	1.62	1.59	1.63	1.59	0.46	
$\text{Lu}(\text{NO}_3)_3$	1.68	1.66	1.69	1.67	0.44	
$\text{Am}(\text{Me}_2\text{PS}_2)(\text{NO}_3)_2$	1.21	1.19	1.28	1.18	0.41	0.96
$\text{La}(\text{Me}_2\text{PS}_2)(\text{NO}_3)_2$	1.34	1.30	1.38	1.29	0.43	0.81
$\text{Eu}(\text{Me}_2\text{PS}_2)(\text{NO}_3)_2$	1.29	1.26	1.32	1.25	0.43	0.86
$\text{Lu}(\text{Me}_2\text{PS}_2)(\text{NO}_3)_2$	1.15	1.13	1.21	1.13	0.41	1.02
$\text{Am}(\text{Me}_2\text{PS}_2)_2(\text{NO}_3)$	0.80	0.76	0.92	0.76	0.34	0.90
$\text{La}(\text{Me}_2\text{PS}_2)_2(\text{NO}_3)$	1.04	1.01	1.12	0.99	0.41	0.78
$\text{Eu}(\text{Me}_2\text{PS}_2)_2(\text{NO}_3)$	0.97	0.94	1.05	0.93	0.41	0.81
$\text{Lu}(\text{Me}_2\text{PS}_2)_2(\text{NO}_3)$	0.67	0.62	0.79	0.62	0.40	0.96
$\text{Am}(\text{Me}_2\text{PS}_2)_3$	0.32	0.25	0.51	0.24		0.86
$\text{La}(\text{Me}_2\text{PS}_2)_3$	0.68	0.67	0.83	0.64		0.77
$\text{Eu}(\text{Me}_2\text{PS}_2)_3$	0.56	0.52	0.73	0.52		0.81
$\text{Lu}(\text{Me}_2\text{PS}_2)_3$	0.20	0.10	0.37	0.10		0.93

^a Calculations were performed using the basis set B1 and ADF program.

Charge Distribution in the Lanthanide Complexes. The trends in Mulliken charges, even though Mulliken charges are known to be strongly basis set dependent,³⁷ for similar species under identical calculation procedures may reflect some physical features. There are literature reports where the metal–ligand bond covalence was estimated from the Mulliken population analysis.^{62,63} Mulliken charge distributions on the metal ions and ligands (nitrate and dithiophosphate) were calculated before

and after complexation, and transfer of Mulliken charges from the ligand to metal ions during complexation was calculated for both the ligands from the difference between the total charge of the ligand (sum of the charges on the constituent atoms of the ligand) in the complex and that of the free ligand which is singly negative in the present work (Table 4). Ligand to metal charge transfer was found to be much lower in the case of NO_3^- as compared to the Me_2PS_2^- ion, which implies a higher degree of covalence in the metal–ligand bond in the case of Me_2PS_2^- ion, and this result is consistent with the higher ΔE_{orb} values with an increasing number of Me_2PS_2^- ions. If we compare the Am^{3+} and Eu^{3+} complexes, higher charge has been transferred from Me_2PS_2^- to Am^{3+} ion as compared to the Eu^{3+} ion leading to less positive charge on Am as compared to Eu. Mulliken charges on Am and the three lanthanides were also calculated using other DFT functionals (PW91, BLYP, and PBE), and in all the cases the charges on Am were less positive as compared to Eu in their complexes with the Me_2PS_2^- ligand (Table 4), indicating a higher degree of covalence in the Am–S bond as compared to the Eu–S bond. More negative enthalpy for Am^{3+} extraction by Cyanex-301 as compared to that for Eu^{3+} extraction observed from the solvent extraction studies also suggests higher covalence in the Am–S bond as compared to the Eu–S bond.^{9,58} This was also supported by the shorter Am–S bond as compared to the Eu–S in the complexes with the Me_2PS_2^- ion (Table 1). Dithiophosphate ligands, therefore, show high selectivity for trivalent Am(III) over the lanthanides.

Effect of Solvent on the Complexation of Am^{3+} , La^{3+} , Eu^{3+} , and Lu^{3+} with Me_2PS_2^- and NO_3^- Ligands. The solvation effect of aqueous soluble species, i.e., M^{3+} ions, NO_3^- ion, and $\text{M}(\text{NO}_3)_3$ complexes, was studied in water, and the organic soluble species, i.e., $\text{M}(\text{Me}_2\text{PS}_2)(\text{NO}_3)_2$, $\text{M}(\text{Me}_2\text{PS}_2)_2(\text{NO}_3)$, and $\text{M}(\text{Me}_2\text{PS}_2)_3$, were studied in toluene medium. In the case of $\text{Am}(\text{Me}_2\text{PS}_2)_3$ and $\text{Eu}(\text{Me}_2\text{PS}_2)_3$ complexes, the geometry optimization was performed both in gas phase and in toluene medium and the changes were insignificant in presence of solvent. The Am–S bond in the complex $\text{Am}(\text{Me}_2\text{PS}_2)_3$ was found to be 2.829 and 2.828 Å, and the Eu–S bond in the $\text{Eu}(\text{Me}_2\text{PS}_2)_3$ complex was 2.860 and 2.856 Å from the gas phase DFT calculations and in presence of solvent. For all the complexes, single point SCF calculations were, therefore, performed in the solvent medium using the gas phase optimized geometries. If we compare the natural charges on Am and Eu in their complexes in gas phase and in the presence of solvent (Table 5), small changes were observed except for the nitrate complexes $\text{M}(\text{NO}_3)_3$ in water medium. The trends, however, did not alter in the presence of solvent, and it is consistent with the Mulliken charges determined from the gas phase calculations (Table 4); i.e., with increasing the number of Me_2PS_2^- ligands, more charge has been transferred from ligand to metal in the case of Am^{3+} as compared to that in the case of Eu^{3+} , resulting in a higher degree of covalence in the Am–S bond as compared to the Eu–S bond. Energies for the complexation in the gas phase ($\Delta E_{\text{n(gas)}}$) and in the presence of water as solvent ($\Delta E_{\text{n(aq)}}$), and the energies for the extraction of metal ion from water (aq) to toluene (tol) medium (ΔE_{ext}), were calculated considering eqs 5–7, respectively, where $n = 0–3$ (Table 6):

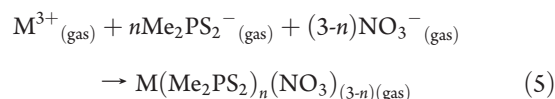


Table 5. Natural Charges on Americium and Europium Calculated by Natural Population Analysis in Their Different Complexes with NO_3^- and Me_2PS_2^- Ligands Both in Gas Phase and in Presence of Solvent [Water for $\text{M}(\text{NO}_3)_3$ and Toluene for Other Complexes] Phase^a

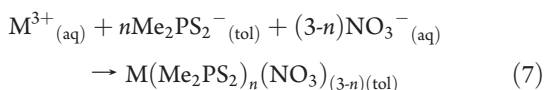
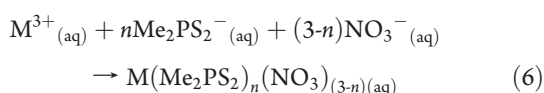
complex	$Q(\text{M})_{\text{gas}}$	$Q(\text{M})_{\text{sol}}$
$\text{Am}(\text{NO}_3)_3$	1.87	1.95
$\text{Eu}(\text{NO}_3)_3$	1.79	1.61
$\text{Am}(\text{Me}_2\text{PS}_2)(\text{NO}_3)_2$	1.49	1.49
$\text{Eu}(\text{Me}_2\text{PS}_2)(\text{NO}_3)_2$	1.48	1.50
$\text{Am}(\text{Me}_2\text{PS}_2)_2(\text{NO}_3)$	1.08	1.09
$\text{Eu}(\text{Me}_2\text{PS}_2)_2(\text{NO}_3)$	1.16	1.16
$\text{Am}(\text{Me}_2\text{PS}_2)_3$	0.65	0.65
$\text{Eu}(\text{Me}_2\text{PS}_2)_3$	0.82	0.83

^a Calculations were performed using the basis set B2 and the exchange-correlation functional BP86 in TURBOMOLE.

Table 6. Complexation Energies (kcal.mol^{-1}) for the Reaction $\text{M}^{3+} + n\text{Me}_2\text{PS}_2^- + (3-n)\text{NO}_3^- \rightarrow \text{M}(\text{Me}_2\text{PS}_2)_n(\text{NO}_3)_{3-n}$ in Gas Phase ($\Delta E_{n(\text{gas})}$) and Water ($\Delta E_{n(\text{aq})}$) and the Energies for Extraction from Water to Toluene (ΔE_{ext})^a

complex	$\Delta E_{n(\text{gas})}$	$\Delta E_{n(\text{aq})}$	ΔE_{ext}	$\Delta E_{r(\text{aq})}$
$\text{Am}(\text{NO}_3)_3$	-1049.6	-156.8	0	0
$\text{La}(\text{NO}_3)_3$	-975.5	-26.0	0	0
$\text{Eu}(\text{NO}_3)_3$	-1069.7	-90.3	0	0
$\text{Lu}(\text{NO}_3)_3$	-1099.7	-35.1	0	0
$\text{Am}(\text{Me}_2\text{PS}_2)(\text{NO}_3)_2$	-1050.7	-160.8	-185.2	-4.0
$\text{La}(\text{Me}_2\text{PS}_2)(\text{NO}_3)_2$	-976.3	-18.3	-39.9	7.7
$\text{Eu}(\text{Me}_2\text{PS}_2)(\text{NO}_3)_2$	-1069.1	-91.6	-115.6	-1.3
$\text{Lu}(\text{Me}_2\text{PS}_2)(\text{NO}_3)_2$	-1098.9	-39.5	-64.7	-4.4
$\text{Am}(\text{Me}_2\text{PS}_2)_2(\text{NO}_3)$	-1047.7	-164.6	-219.4	-7.8
$\text{La}(\text{Me}_2\text{PS}_2)_2(\text{NO}_3)$	-974.7	-20.0	-73.9	6.0
$\text{Eu}(\text{Me}_2\text{PS}_2)_2(\text{NO}_3)$	-1065.3	-93.8	-148.6	-3.5
$\text{Lu}(\text{Me}_2\text{PS}_2)_2(\text{NO}_3)$	-1093.7	-42.3	-97.1	-7.2
$\text{Am}(\text{Me}_2\text{PS}_2)_3$	-1042.0	-166.3	-251.2	-9.5
$\text{La}(\text{Me}_2\text{PS}_2)_3$	-971.0	-23.2	-107.3	2.8
$\text{Eu}(\text{Me}_2\text{PS}_2)_3$	-1059.3	-94.9	-180.0	-4.6
$\text{Lu}(\text{Me}_2\text{PS}_2)_3$	-1084.7	-41.1	-125.8	-6.0

^a Calculations were performed using the basis set B2 and the exchange-correlation functional BP86 in TURBOMOLE.



The lower ΔE values in the presence of solvent as compared to the gas phase results is due to the requirement of high dehydration energy prior to the complexation in the presence of solvent. The reaction energies ($\Delta E_{r(\text{aq})} = \Delta E_{n(\text{aq})} - \Delta E_{0(\text{aq})}$) in aqueous medium were also calculated and shown in Table 6. Similar

trends as gas phase calculations were observed in the presence of solvent in the ΔE_r values. ΔE_n values, however, show different trends in the presence of solvent, and it was found to be more favorable for the Am^{3+} complexes as compared to the Eu^{3+} complexes. This may also be responsible for the selectivity of dithiophosphinate ligands for Am^{3+} over Eu^{3+} as described by Cao et al. for the selective complexation of Am^{3+} by bis(2,4,4-trimethylpentyl)dithiophosphinic acid in the presence of solvent.²¹ In all these calculations, the COSMO approach is used and treatment of water molecules explicitly may give a clearer picture of the solvent effect, which, of course, is computationally challenging for these large complexes.

CONCLUSIONS

In the solvent extraction study, Am^{3+} and Lu^{3+} were extracted by Cyanex-301 as MA_3 and $\text{MA}_2(\text{NO}_3)$ types of complexes, respectively, irrespective of Cyanex-301 concentration, whereas in the case of La^{3+} and Eu^{3+} , the extractable species changes from $\text{MA}_2(\text{NO}_3)$ to MA_3 depending on the Cyanex-301 concentration used. This was explained on the basis of energies required to form the respective species from their corresponding trinitrate complexes, which were calculated using the density functional method using four different GGA functionals. The calculated metal–ligand complex formation energies were partitioned into various components like orbital and steric interactions. Higher covalent character in the M–S bond in the dithiophosphinate complexes as compared to the M–O bond in the nitrate complexes was reflected in higher orbital (ΔE_{orb}) and lower electrostatic (ΔE_{elec}) interactions for the complexes with a greater number of Me_2PS_2^- ions. The ΔE_n or ΔE_{int} values were not favorable for Am^{3+} complexes as compared to the Eu^{3+} complexes in the gas phase studies. The higher selectivity of the dithiophosphinate ligands for Am^{3+} over Eu^{3+} cannot, therefore, be attributed only to the marginally higher covalence in the Am–S bond as compared to the Eu–S bond as seen from the shorter Am–S bond and higher ligand to metal charge transfer in the dithiophosphinate complexes of Am^{3+} . More favorable ΔE_n or ΔE_{int} values for the Am^{3+} complexes in the presence of solvent also play an important role in controlling the selectivity of dithiophosphinate ligands for Am^{3+} over Eu^{3+} . These observations were consistent with different functionals used for the gas phase DFT calculations as well as in presence of solvents.

AUTHOR INFORMATION

Corresponding Author

*E-mail: mpatra@barc.gov.in (P.K.M.). Fax: +91-22- 25505151.

REFERENCES

- (1) Mathur, J. N.; Murali, M. S.; Nash, K. L. *Solvent Extr. Ion Exch.* **2001**, *19*, 357.
- (2) Purroy, D. S.; Baron, P.; Christiansen, B.; Glatz, J. P.; Madic, C.; Malmbeck, R.; Modolo, G. *Sep. Purif. Technol.* **2005**, *45*, 157.
- (3) Diamond, R. M.; Street, K., Jr.; Seaborg, G. T. *J. Am. Chem. Soc.* **1954**, *76*, 1461.
- (4) Moore, F. L. *Anal. Chem.* **1961**, *33* (6), 749.
- (5) Moore, F. L. *Anal. Chem.* **1964**, *36* (11), 2159.
- (6) Baybarz, R. D.; Weaver, B. S.; Kinser, H. B. *Nucl. Sci. Eng.* **1963**, *17*, 457.
- (7) Musikas, C.; Cuillerdier, C.; Livet, J.; Forchioni, A.; Chachaty, C. *Inorg. Chem.* **1983**, *22* (18), 2513.

- (8) Madic, C.; Hudson, M. J.; Liljenzin, J. O.; Glatz, J. P.; Nannicini, R.; Facchini, A.; Kolarik, Z.; Odoj, R. *New Partitioning Techniques for Minor Actinides, European Commission Report, EUR 19149*; European Union: Brussels, 2000.
- (9) Zhu, Y.; Chen, J.; Jiao, R. *Solvent Extr. Ion Exch.* **1996**, *14*, 61.
- (10) Modolo, G.; Odoj, R. *J. Radioanal. Nucl. Chem.* **1998**, *228* (1–2), 83.
- (11) Wei, Y.; Kumagai, M.; Takashima, Y.; Modolo, G.; Odoj, R. *Nucl. Technol.* **2000**, *132*, 413.
- (12) Bhattacharyya, A.; Mohapatra, P. K.; Ansari, S. A.; Raut, D. R.; Manchanda, V. K. *J. Membr. Sci.* **2008**, *312*, 1.
- (13) Hill, C.; Madic, C.; Baron, P.; Ozawa, M.; Tanaka, Y. *J. Alloys Compd.* **1998**, *271–173*, 159.
- (14) Ionova, G.; Ionov, S.; Rabbe, C.; Hill, C.; Madic, C.; Guillaumont, R.; Krupa, J. C. *Solvent Extr. Ion Exch.* **2001**, *19* (3), 391.
- (15) Bhattacharyya, A.; Mohapatra, P. K.; Manchanda, V. K. *Solvent Extr. Ion Exch.* **2006**, *24*, 1.
- (16) Jensen, M. P.; Bond, A. H. *J. Am. Chem. Soc.* **2002**, *124*, 9870.
- (17) Tian, G.; Zhu, Y.; Xu, J.; Zhang, P.; Hu, T.; Xie, Y.; Zhang, J. *Inorg. Chem.* **2003**, *42*, 735.
- (18) Boehme, C.; Wipff, G. *Inorg. Chem.* **1999**, *38*, 5734.
- (19) Boehme, C.; Wipff, G. *Chem.—Eur. J.* **2001**, *7* (7), 1398.
- (20) Coupez, B.; Boehme, C.; Wipff, G. *J. Phys. Chem. B* **2003**, *107*, 9484.
- (21) Cao, X.; Heidelberg, D.; Ciupka, J.; Dolg, M. *Inorg. Chem.* **2010**, *49*, 10307.
- (22) Bhattacharyya, A.; Mohapatra, P. K.; Manchanda, V. K. *Solvent Extr. Ion Exch.* **2007**, *25*, 27.
- (23) Mohapatra, P. K. Ph.D. Thesis, University of Bombay, 1993
- (24) Petit, L.; Daul, C.; Adamo, C.; Maldivi, P. *New J. Chem.* **2007**, *31*, 1738.
- (25) Petit, L.; Adamo, C.; Maldivi, P. *Inorg. Chem.* **2006**, *45*, 8517.
- (26) Miguiditchian, M.; Guillaneux, D.; Moisy, P.; Madic, C.; Jensen, M. P.; Nash, K. L. *Inorg. Chem.* **2005**, *44*, 1404.
- (27) Becke, A. D. *Phys. Rev. A: At, Mol, Opt. Phys.* **1988**, *38*, 3098.
- (28) Perdew, J. P. *Phys. Rev. B: Condens. Matter Mater. Phys.* **1986**, *33*, 8822.
- (29) Austin, J. P.; Burton, N. A.; Hiller, I. H.; Sundarajan, M.; Vincent, M. A. *Phys. Chem. Chem. Phys.* **2009**, *11*, 1143.
- (30) Wählin, P.; Danilo, C.; Vallet, V.; Réal, F. J.; Wahlgreen, U. *J. Chem. Theory Comput.* **2008**, *4*, 569.
- (31) Vetere, V.; Roos, B. O.; Maldivi, P.; Adamo, C. *Chem. Phys. Lett.* **2004**, *396*, 452.
- (32) Vetere, V.; Maldivi, P.; Adamo, C. *J. Comput. Chem.* **2003**, *24* (7), 850.
- (33) Perdew, J. P.; Chevary, J. A.; Vosko, S. H.; Jackson, K. A.; Pederson, M. R.; Singh, D. J.; Fiolhais, C. *Phys. Rev. B: Condens. Matter Mater. Phys.* **1992**, *46*, 6671.
- (34) Lee, C.; Yang, W.; Parr, R. G. *Phys. Rev. B: Condens. Matter Mater. Phys.* **1988**, *37* (2), 785.
- (35) Perdew, J. P.; Burke, K.; Ernzerhof, M. *Phys. Rev. Lett.* **1996**, *77*, 3865.
- (36) Snijders, J. G.; Baerends, E. J.; Vernooijs, P. *At. Data Nucl. Data Tables* **1982**, *26*, 483.
- (37) Chang, C.; Pelissier, M.; Durand, Ph. *Phys. Scr.* **1986**, *34*, 394.
- (38) Heully, J.-L.; Lindgren, I.; Lindroth, E.; Lundquist, S.; Martensson-Pendrill, A.-M. *J. Phys. B* **1986**, *19*, 2799.
- (39) van Lenthe, E.; Baerends, E. J.; Snijders, J. G. *J. Chem. Phys.* **1993**, *99*, 4597.
- (40) van Lenthe, E.; Baerends, E. J.; Snijders, J. G. *J. Chem. Phys.* **1996**, *105*, 6505.
- (41) van Lenthe, E.; van Leeuwen, R.; Baerends, E. J.; Snijders, J. G. *Int. J. Quantum Chem.* **1996**, *57*, 281.
- (42) te Velte, G.; Bickelhaupt, F. M.; van Gisbergen, S. A.; Fonseca Guerra, C.; Baerends, E. J.; Snijders, J. G.; Ziegler, T. *J. Comput. Chem.* **2001**, *22* (9), 931.
- (43) Fonseca Guerra, C.; Snijders, J. G.; te Velte, G.; Baerends, E. J. *Theor. Chem. Acc.* **1998**, *391*.
- (44) *ADF2006.01, SCM*; Theoretical Chemistry, Vrije Universiteit: Amsterdam, The Netherlands; <http://www.scm.com>.
- (45) Guillaumont, D. *J. Phys. Chem. A* **2004**, *108*, 6893.
- (46) Kaltsoyannis, N. *Chem. Soc. Rev.* **2003**, *32*, 9.
- (47) Ziegler, T.; Rauk, A. *Theor. Chim. Acta* **1977**, *46*, 1.
- (48) Klamt, A.; Schuurmann, G. *J. Chem. Soc., Perkin Trans.* **1993**, *2*, 799.
- (49) TURBOMOLE is program package developed by the Quantum Chemistry Group at the University of Karlsruhe, Germany, 1988. Ahlrichs, R.; Bär, M.; Häser, M.; Horn, H.; Kölmel, C. *Chem. Phys. Lett.* **1989**, *162*, 165.
- (50) Kuechle, W.; Dolg, M.; Stoll, H.; Preuss, H. *J. Chem. Phys.* **1994**, *100*, 7535.
- (51) Cao, X.; Dolg, M.; Stoll, H. *J. Chem. Phys.* **2003**, *118*, 487.
- (52) Cao, X.; Dolg, M. *THEOCHEM* **2004**, *673*, 203.
- (53) Dolg, M.; Stoll, H.; Preuss, H. *J. Chem. Phys.* **1989**, *90*, 1730.
- (54) Cao, X.; Dolg, M. *J. Chem. Phys.* **2001**, *115*, 7348.
- (55) Cao, X.; Dolg, M. *THEOCHEM* **2002**, *581*, 139.
- (56) Dolg, M.; Stoll, H.; Preuss, H. *Theor. Chim. Acta* **1993**, *85*, 441.
- (57) Cosentino, U.; Villa, A.; Pitea, D.; Moro, G.; Barone, V. *J. Phys. Chem. B* **2000**, *104*, 8001.
- (58) Bhattacharyya, A.; Mohapatra, P. K.; Manchanda, V. K. *Radiochim. Acta* **2010**, *98*, 141.
- (59) Dobler, M.; Guilbaud, P.; Dedieu, A.; Wipff, G. *New J. Chem.* **2001**, *25*, 1458–1465.
- (60) Shannon, R. *Acta Crystallogr.* **1976**, *A32*, 751.
- (61) Kuchen, W.; Hertel, H. *Angew. Chem., Int. Ed. Engl.* **1969**, *8* (2), 89.
- (62) Guillaumont, D. *THEOCHEM* **2006**, *771*, 105.
- (63) Maldivi, P.; Petit, L.; Adamo, C.; Vetere, V. *C. R. Chim.* **2007**, *10*, 888.